Tailoring Architecture of Nanothin Hydrogels: Effect of Layering on pH-Triggered Swelling

Veronika Kozlovskaya,[†] Oleksandra Zavgorodnya,[†] Yun Wang,[†] John F. Ankner,*[‡] and Eugenia Kharlampieva*[†]

[†]Department of Chemistry, University of Alabama at Birmingham, Birmingham, Alabama, 35294, United States
[‡]Oak Ridge National Laboratory, Oak Ridge, Tennessee 37831, United States

S *Supporting Information*

ABSTRACT: We have tailored the internal architecture of ultrathin poly(methacrylic acid) (PMAA) hydrogels from well stratified to highly intermixed by controlling the internal structure in layer-by-layer templates used for hydrogel fabrication. We have found pH-triggered swelling properties of these hydrogels to be significantly affected by hydrogel architecture. Well-stratified hydrogels exhibited a dramatic 10-fold increase in thickness when transitioned between pH = 5 and 7.5, unlike the 2-fold swelling observed in less-organized hydrogels.
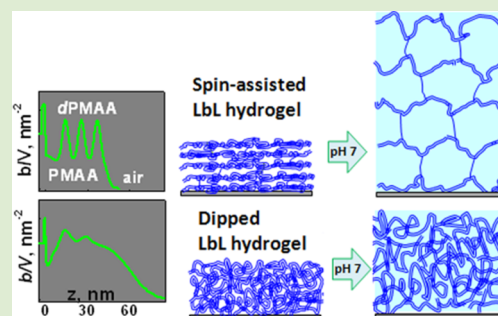
Hydrogels, or cross-linked polymeric networks, are capable of significant water uptake and have numerous applications in drug delivery, tissue engineering, and sensing.[1] Stimuli-responsive hydrogels are particularly appealing. Stimuli-triggered swelling/shrinking can be tuned by changing hydrogel mesh size, composition, and thickness.[2,3] Recently introduced layer-by-layer (LbL)-derived hydrogels offer systems of nanoscale thickness (<100 nm).[4] LbL assembly performed via alternating adsorption of polymers at surfaces enables fabrication of films on almost any substrate with nanoscale control over film composition, structure, and properties.[5] LbL-based hydrogels were produced by cross-linking both during and post-assembly.[6] In the latter case, templates of hydrogen-bonded or ionically paired LbL films were exposed to thermal, photo, or chemical cross-linking conditions.[4a,c,d] The stimuli-triggered behaviors of those systems were provided by functional groups not involved in covalent binding. Unlike "bulk" macro- and microgels, nanothin hydrogels enable fast response, a feature crucial for sensing and drug delivery.[1,4d] Hydrogel architecture originating from chain arrangements in a network has been found to greatly affect the morphology and properties of "bulk" hydrogels.[7] Hydrogel architecture on a microscale has proven useful for regulating cell differentiation and migration in vitro and in vivo.[7b] Controlling the microstructure of cellulose-based macrogels has been crucial to achieving high water uptake and tunable mechanical properties.[8] Much less is known about the internal structure of nanothin networks. Ultrathin multilayer-derived hydrogels have been investigated for responsiveness by varying chemical composition, assembly routes, and charge balance, rather than internal organization.[4,9,10] The absence of studies on hydrogel architecture is due at least partly to the difficulty of controlling

the structural organization of randomly chemically linked networks. Another challenge is the inability of conventional instrumental tools to resolve internal structure at the nanoscale. This lack of knowledge prevents rational design of surface nanogels with predictable and easily tunable properties.

In the present study, we demonstrate a first example of tuning swelling of ultrathin hydrogels by controlling internal structure. Highly swollen hydrogels, which swell up to 18 times the original dry thickness at pH = 7.5, are obtained from well-stratified "spin-assisted" templates; while 3 times lower swelling is displayed by intermixed "dipped" precursors. Regulating swelling behavior of stimuli-responsive hydrogels at the nanoscale is crucial for developing advanced drug delivery and sensing applications.

The hydrogel films investigated here involve pH-sensitive poly(methacrylic acid) (PMAA) networks produced by chemical cross-linking of PMAA layers in hydrogen-bonded multilayer templates. Although PMAA-based hydrogels have been investigated,[4c,9] including recently by our group,[11] there are no studies on regulating the internal structure of such systems and the effect on hydrogel swelling. Because ultrathin multilayer-derived hydrogels have shown considerable promise in controlled drug release; cellular, protein, or bacterial adhesion[12–14] and inkjet printing,[4a] structural information about such films is highly relevant.

To probe hydrogel architecture, neutron reflectivity (NR) was utilized. This technique exploits the neutron scattering contrast between the proton and the deuteron and has been
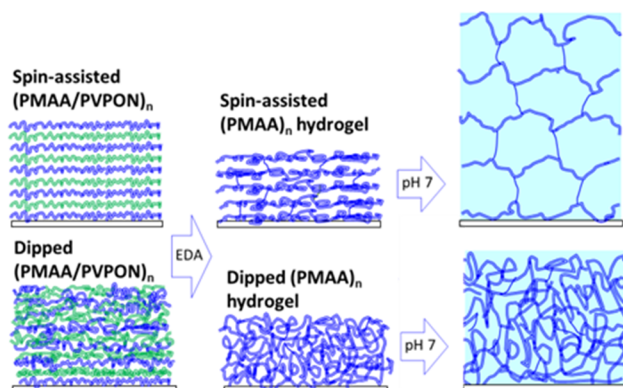
successfully employed to probe internal structures of biomimetic films and hydrogen-bonded and ionically bound multilayers as well as their swelling.[15−21]

Hydrogel fabrication is schematically illustrated in Figure 1. First, hydrogen-bonded templates were produced by alternating


Figure 1. pH-responsive (PMAA)$_n$ hydrogels produced by chemical cross-linking of spin-assisted and dipped (PMAA/PVPON)$_n$ hydrogen-bonded precursors.

deposition of PMAA (M_w = 150000 g/mol) with poly(N-vinylpyrrolidone) (PVPON, M_w = 55000 g/mol) on 2 in. diameter Si wafers from 1 mg/mL solutions in 10 mM phosphate buffer at pH 2.5. The Si wafers were primed with a 3.5-bilayer (PAH/PSS) film of 5 nm dry thickness to enhance adhesion. Deuterated PMAA (dPMAA, M_w = 198000 g/mol) was deposited with every fifth bilayer to provide neutron contrast. The neutron refractive index derives from the product of the density of nuclei in space and their individual scattering amplitudes. The deuteron looks different than the proton and this scattering contrast is used to highlight selected layers. These hydrogen-bonded multilayers were then treated with ethylenediamine to cross-link PMAA layers, followed by PVPON release at basic pH and formation of [(PMAA)$_4$dPMAA]$_3$(PMAA)$_2$ networks. Here, PVPON was used as a sacrificial binder to assemble the hydrogen-bonded multilayer.

Hydrogel architecture is defined by the internal structure of the initial hydrogen-bonded templates. To elucidate the effect of deposition conditions on multilayer architecture, spin-assisted and conventional "dipping" LbL depositions were performed (see SI). As confirmed with ellipsometry and in situ attenuated total reflection Fourier transform infrared spectroscopy (ATR-FTIR), the multilayers grow linearly, which correlates well with earlier studies of electrostatically bound films produced by both methods (Figure S1).[20b]

Measured neutron reflectivity of a spin-assisted hydrogen-bonded film is shown in Figure 2a,b. Normalized neutron reflectivity RQ^4 is plotted versus wavevector transfer Q ($Q = 4\pi \sin \theta/\lambda$, where λ is the neutron wavelength and θ the incident angle). The quality of layer ordering revealed by the spacing between deuterated marker layers is manifested in superlattice peaks in the NR profiles.[15,22] The as-deposited film shows a high degree of stratification illustrated by a strong first-order Bragg peak near $Q = 0.36$ nm^{-1}. The fitted scattering-length-density (SLD) profile reveals a well-defined and equally spaced sequence of labeled dPMAA layers (Figure 2b). The labeled layers are 3.3 nm in thickness and well-separated by 12.1 nm of
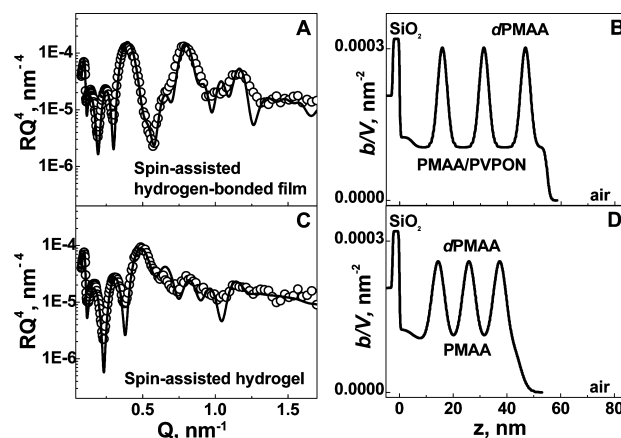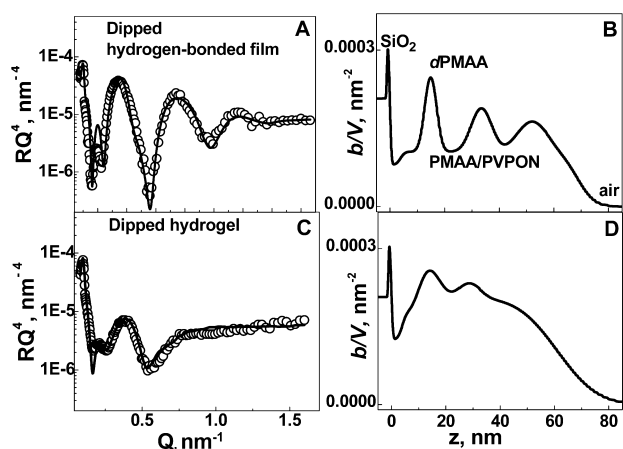

Figure 2. Normalized NR data (A, C) and corresponding SLD profiles (B, D) for a spin-assisted dry film before (A, B) and after (C, D) cross-linking. Open symbols and solid lines show experimental NR data and fit, respectively.

protonated material. Scattering parameters for the NR fits are listed in the SI.

The hydrogen-bonded multilayer was converted into a cross-linked PMAA network by treatment with ethylenediamine at pH = 5.8 for 16 h (see SI).[9,11] Post-cross-link neutron reflectivity data is shown in Figure 2c,d. The presence of distinct, periodic, and sharply contrasting dPMAA layers in the fitted SLD profile is striking (Figure 2d), indicating that layering is preserved in the hydrogel. However, the SLDs of the dPMAA layers decreased from 3.6×10^{-4} nm^{-2} before cross-linking to 3.1×10^{-4} nm^{-2} after cross-linking, indicating increased intermixing of dPMAA with hydrogenated material (Tables 2 and 3, SI. Despite this diffusion, the three marker layers are well separated without any degradation in layering. Internal roughness is constant throughout the film, increasing from 3.3 to 4.2 nm upon cross-linking, while the external roughness increased from 2 to 5.5 nm (Table 1, SI).

In drastic contrast, when conventional dipping was employed, the hydrogen-bonded film displayed a significant decay in layering. The SLD profile of this film exhibits a gradual decrease in peak height and increased broadening away from the substrate, indicating significant layer intermixing upon successive dipping steps (Figure 3b). Substantial layer interpenetration in the dipped (PVPON/PMAA) films was seen previously and was explained by weak intermolecular interactions.[20] Importantly, these results demonstrate that hydrogen-bonded films can exhibit a higher degree of layer ordering when assembled by the spin-assisted method. This observation correlates well with data reported previously for spin-assisted films of ionically paired and hydrogen-bonded multilayers.[22−24] Those films showed a high degree of stratification, unlike comparable highly intermixed dipped films. Shear forces and fast solvent removal seem to trap polymer chains and limit their reorganization during spin-assisted assembly.[23]
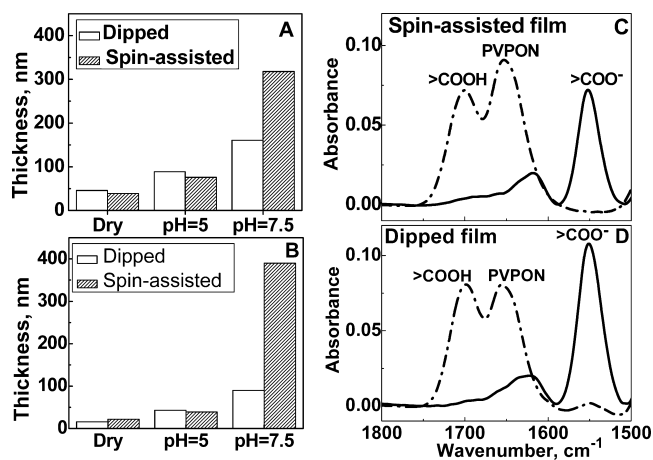
Neutron reflectivity data for a dipped hydrogel evince extreme layer interpenetration indicated by the significant dilution of dPMAA (Figure 3c,d). The fitted SLD profile exhibits strong intermixing, grading to near-complete dissolution at the film surface (Figure 3d). The values of internal and external roughness are significantly larger than those for spin-assisted hydrogels, progressing from 7.4 nm within the film to up to 27 nm at the surface (Table 1, SI).

Figure 3. Normalized NR data (A, C) and corresponding SLD profiles (B, D) for dipped dry film before (A, B) and after (C, D) cross-linking. Open symbols and solid lines represent experimental NR data and fit, respectively.

Figure 4. (A, B) Thickness variations of spin-assisted and dipped hydrogels in dry states and in solutions at pH = 5 and pH = 7.5. (C, D) FTIR spectra of spin-assisted (C) and dipped films (D) as cast (dashed curves) and after cross-linking (solid curve), as monitored by in situ ATR-FTIR in D_2O solutions. Absorption bands associated with protonated carboxylic groups (−COOH), ionized carboxylic groups (−COO⁻), and carbonyl vibration band of PVPON are centered at 1700, 1550, and 1650 cm⁻¹, respectively.

Cross-linking either type of hydrogen-bonded film results in increased layer interpenetration, a decrease in SLD contrast, and increased internal and external roughness. However, the spin-assisted hydrogels are much better stratified than the dipped. Importantly, spin-assisted hydrogels preserved the initial periodicity of the marker layers, despite having partially mixed interfaces. Strikingly, PVPON release upon cross-linking does not disturb layer ordering. In contrast, the architecture of the dipped films was affected by cross-linking more severely, resulting in a highly disordered film with significantly larger external roughness than before cross-linking. The more disordered structure of the dipped hydrogel evolves from the weakly ordered as-grown hydrogen-bonded templates. Loss of internal structure upon release of one of the film components was observed earlier in dipped electrostatically bound films. There, selective release of PMAA induced by elevated pH totally destroyed layering in QPVP/PMAA multilayers, as they were not cross-linked and so lacked any constraint to internal QPVP rearrangement.[19]

Finally, we have found using liquid ellipsometry that spin-assisted and dipped hydrogels exhibit drastically different swelling behaviors. A spin-assisted hydrogel, 39 nm thick dry, swells to 8 times its dry thickness in pH = 7.5, indicating 90 v/v % of water in the swollen ionic film (Figure 4a). In contrast, a dipped 46-nm film swells to 3 times its original dry thickness in pH = 7.5. Spin-assisted and dipped hydrogels exhibit pH-triggered shrinkage/swelling as a result of protonation/ionization of PMAA carboxylic groups. The spin-assisted film exhibits a 4-fold increase in thickness between pH = 5 and 7.5, compared with a 2-fold swelling in dipped hydrogels. We also found that thinner hydrogels follow the same trend. A spin-assisted 22-nm dry hydrogel swelled to 39 nm and then to 390 nm at pH = 5 and 7.5, respectively, a 10-fold increase (Figure 4b). Greater swelling of thin hydrogels compared to the thicker films was observed earlier with dimethylacrylamide networks and attributed to the preferential swelling of such films in one dimension due to surface-induced constraints.[25] This hydrogel represents a unique example of an ultrathin but highly swollen film capable of a dramatic 18-fold increase in thickness upon hydration (94% water uptake) at pH 7.5 (Figure 4b). In contrast, a dipped film of similar thickness swells ~5 times its original dry thickness in pH 7.5, exhibiting only a 2-fold increase in thickness between pH = 5 and 7.5. These data on dipped systems are consistent with previously reported swelling ratios of dipped multilayer PMAA networks found to fall in a range from 1.4 to 2.5, depending on cross-linking time.[9,26] These results also agree with our previous findings on dipped multilayer PMAA hydrogels cross-linked with EDC.[11b]

Our results indicate that well-structured spin-assisted hydrogels have greater free volume at pH = 7.5 than their less-organized dipped counterparts. To quantify this difference, cross-link densities and network mesh sizes were derived using in situ ATR-FTIR and ellipsometry. Figure 4c,d demonstrates ATR-FTIR spectra of both spin-assisted and dipped systems before and after cross-linking. The spectra confirm no mass loss of PMAA but the disappearance of PVPON and appearance of amide peaks after cross-linking. The difference ratio between amide-peak fraction integrated intensities for spin-assisted and dipped hydrogels is 0.11, implying there were only 11% more carboxyl groups in the spin-assisted hydrogel involved in amide bond formation than in dipped hydrogels.

The cross-link density of dipped hydrogels was calculated from experimental data on hydrogel swelling at pH = 5 using the Flory equation for one-dimensional swelling of nonionic gels.[11b,26] Considering the ratio of dry to swollen hydrogel thicknesses $\phi_2 = (46/90) = 0.513$, and PMAA $M_w = 150000$ g/mol, the calculation yielded, on average, 7.3 ± 0.5 monomer units between cross-links in the dipped hydrogels (see SI). Accounting for the 11% difference found with ATR-FTIR, the cross-link density in the spin-assisted hydrogel was calculated to be similar, resulting in 6.5 ± 0.4 monomer units. From the known cross-link density, we estimated the mesh size m for the polymer network in dipped and spin-assisted hydrogels using eq 1:

$$m = \phi_2^{-1/3} C_n^{1/2} n^{1/2} l \qquad (1)$$

in which, C_n is the characteristic ratio of the polymer (14.6 for PMAA),[27] n is the number of bonds between cross-links (n = 14.6 and 13 for dipped and spin-assisted hydrogels, respectively), and l is the C−C bond length (0.154 nm). For

the dipped hydrogel film, the mesh sizes were estimated to be 2.8 and 3.4 nm for pH = 5 and 7.5, respectively. In contrast, the mesh sizes in the spin-assisted hydrogel were estimated to be 2.7 and 4.3 nm for pH = 5 and 7.5, respectively (see SI for details).

Our results indicate that despite similar cross-link densities, there is a significant difference in the mesh sizes of spin-assisted and dipped hydrogels. Indeed, spin-assisted hydrogels exhibited a 60% increase in the mesh size between pH = 5 and 7.5, while only a 21% increase is observed for dipped films under the same conditions. This result correlates well with a 3-fold greater swelling of spin-assisted hydrogels at pH = 7.5. We suggest that this difference in swelling arises from the difference in chain conformations during assembly. Intuitively, chain mobility and the corresponding free volume in the hydrogel is controlled by chain conformations adopted during both deposition and cross-linking steps, as well as by chain rearrangements in response to external stimuli. During spin-assisted assembly, polymer chains are deposited in a mobility-limited state.[22,23,28] As a result, layers are composed of "frozen" chains deposited in loops and tails without much intermixing with the neighboring layers, yielding a highly stratified, cross-linked network. These loops and entanglements expand at high pH, providing the needed free volume for swelling. In contrast, in the dipped films, polymer chains are more interdiffused as a result of chain exchange during assembly. These chain entanglements decrease free volume in the dipped hydrogels, significantly constraining hydrogel swelling.

In conclusion, we have demonstrated that internal film structure of ultrathin surface hydrogels is strongly correlated with the architecture of the as-deposited hydrogen-bonded films, which in turn depends on deposition conditions. We also have shown that hydrogel swelling is strongly influenced by network architecture. An intriguing question posed by the current work is the internal structure of these hydrogels in the pH-swollen state, study of which is currently underway.

■ ASSOCIATED CONTENT

ⓢ Supporting Information

Contains experimental details on hydrogel cross-linking, ellipsometry, in situ ATR-FTIR, and NR, and calculation of the cross-link densities and mesh size of hydrogels. This material is available free of charge via the Internet at http://pubs.acs.org.

■ AUTHOR INFORMATION

Corresponding Author

*E-mail: ekharlam@uab.edu; anknerjf@ornl.gov.

Notes

The authors declare no competing financial interest.

■ ACKNOWLEDGMENTS

■ REFERENCES

(1) Tokarev, I.; Minko, S. *Adv. Mater.* **2009**, *21*, 241.

(2) Osada, Y.; Gong, J. P.; Tanaka, Y. *J. Macromol. Sci., Part C: Polym. Rev.* **2004**, *44*, 87.

(3) Zeng, J.; Tikare, V.; Jacob, K. I. *Langmuir* **2006**, *22*, 1333.

(4) (a) Yang, S. Y.; Rubner, M. F. *J. Am. Chem. Soc.* **2002**, *124*, 2100. (b) Serizawa, T.; Matsukuma, D.; Nanameki, K.; Uemura, M.; Kurusu, F.; Akashi, M. *Macromolecules* **2004**, *37*, 6531. (c) Zelikin, A. N.; Li, Q.; Caruso, F. *Chem. Mater.* **2008**, *20*, 2655. (d) Kozlovskaya, V.; Kharlampieva, E.; Erel, I.; Sukhishvili, S. A. *Soft Matter* **2009**, *5*, 4077.

(5) *Multilayer Thin Films: Sequential Assembly of Nanocomposite Materials*; Decher, G., Schlenoff, J., Eds.; Wiley & Sons: New York, 2012.

(6) Rydzek, G.; Schaaf, P.; Voegel, J.-C.; Jierry, L.; Boulmedais, F. *Soft Matter* **2012**, *8*, 9738.

(7) (a) Ladet, S.; David, L.; Domard, A. *Nature* **2008**, *452*, 76. (b) Dai, H.; Li, X.; Long, Y.; Wu, J.; Liang, S.; Zhang, X.; Zhao, N.; Xu, J. *Soft Matter* **2009**, *5*, 1987. (c) Johnson, L. M.; DeForest, C. A.; Pendurti, A.; Anseth, K. S.; Bowman, C. N. *ACS Appl. Mater. Interfaces* **2010**, *2*, 1963. (d) Kizilel, S.; Sawardecker, E.; Teymour, F.; Perez-Luna, V. H. *Biomaterials* **2006**, *27*, 1209.

(8) Appel, E. A.; Loh, X. J.; Jones, S. T.; Biedermann, F.; Dreiss, C. A.; Scherman, O. A. *J. Am. Chem. Soc.* **2012**, *134*, 11767.

(9) Kozlovskaya, V.; Kharlampieva, E.; Mansfield, M. L.; Sukhishvili, S. A. *Chem. Mater.* **2006**, *18*, 328.

(10) Tokarev, I.; Minko, S. *Adv. Mater.* **2010**, *22*, 3446.

(11) (a) Kozlovskaya, V.; Higgins, W.; Chen, J.; Kharlampieva, E. *Chem. Commun.* **2011**, *47*, 8352. (b) Kozlovskaya, V.; Wang, Y.; Higgins, W.; Chen, J.; Chen, Y.; Kharlampieva, E. *Soft Matter* **2012**, *8*, 9828.

(12) Lee, D.; Cohen, R. E.; Rubner, M. F. *Langmuir* **2005**, *21*, 9651.

(13) Yang, S. Y.; Lee, D.; Cohen, R. E.; Rubner, M. F. *Langmuir* **2004**, *20*, 5978.

(14) Akiyama, Y.; Kikuchi, A.; Yamato, M.; Okanto, T. *Langmuir* **2004**, *20*, 5506.

(15) (a) Schmitt, J.; Grünewald, T.; Decher, G.; Pershan, P. S.; Kjaer, K.; Lösche, M. *Macromolecules* **1993**, *26*, 7058. (b) Kellogg, G. J.; Mayes, A. M.; Stockton, W. B.; Ferreira, M.; Rubner, M. F.; Satija, S. K. *Langmuir* **1996**, *12*, 5109. (c) Lösche, M.; Schmitt, J.; Decher, G.; Bouwman, W. G.; Kjaer, K. *Macromolecules* **1998**, *31*, 8893.

(16) (a) Miller, C. E.; Majewski, J.; Faller, R.; Satija, S.; Kuhl, T. L. *Biophys. J.* **2004**, *86*, 3700. (b) Jablin, M. S.; Dubey, M.; Zhernenkov, M.; Toomey, R.; Majewski, J. *Biophys. J.* **2011**, *101*, 128.

(17) Gopinadhan, M.; Ivanova, O.; Ahrens, H.; Günther, J.-U.; Steitz, R.; Helm, C. A. *J. Phys. Chem. B* **2007**, *111*, 8426.

(18) Jomaa, H. W.; Schlenoff, J. B. *Macromolecules* **2005**, *38*, 8473.

(19) Kharlampieva, E.; Ankner, J. F.; Rubinstein, M.; Sukhishvili, S. A. *Phys. Rev. Lett.* **2008**, *100*, 128303.

(20) Kharlampieva, E.; Kozlovskaya, V.; Ankner, J. F.; Sukhishvili, S. A. *Langmiur* **2008**, *24*, 11346. (b) Kharlampieva, E.; Kozlovskaya, V.; Chan, J.; Ankner, J. F.; Tsukruk, V. V. *Langmuir* **2009**, *25*, 14017.

(21) (a) Kolasinska, M.; Krastev, R.; Gutberlet, T.; Warszynski, P. *Langmuir* **2009**, *25*, 1224. (b) Dodoo, S.; Steitz, R.; Laschewsky, A.; von Klitzing, R. *Phys. Chem. Chem. Phys.* **2011**, *13*, 10318. (c) Köhleree, R.; Dönch, I.; Ott, P.; Laschewsky, A.; Fery, A.; Krastev, R. *Langmuir* **2009**, *25*, 11576.

(22) Kozlovskaya, V.; Ankner, J. F.; O'Neill, H.; Zhang, Q.; Kharlampieva, E. *Soft Matter* **2011**, *7*, 11453.

(23) Cho, J.; Char, K.; Hong, J.-D.; Lee, K.-B. *Adv. Mater.* **2001**, *13*, 1076.

(24) Chiarelli, P. A.; Johal, M. S.; Casson, J. L.; Roberts, J. B.; Robinson, J. M.; Wang, H.-L. *Adv. Mater.* **2001**, *13*, 1167.

(25) Toomey, R.; Freidank, D.; Rühe, J. *Macromolecules* **2004**, *37*, 882.

(26) Kharlampieva, E.; Erel-Unal, I.; Sukhishvili, S. A. *Langmuir* **2007**, *23*, 175.

(27) Bell, C. L.; Peppas, N. A. *J. Controlled Release* **1996**, *39*, 201.

(28) Seo, J.; Lutkenhaus, J. K.; Kim, J.; Hammond, P. T.; Char, K. *Langmuir* **2008**, *24*, 995.